Organic Magnets

DOI: 10.1002/anie.200803249

Structural Study of a Dimerization Process in an Organic Radical Magnet, BBDTA·$InBr_4$**

Wataru Fujita, Koichi Kikuchi, and Kunio Awaga*

The time required for the formation and dissociation of bonds in chemical processes, either in gaseous or in condensed phases, is usually very short.[1] Therefore, it is difficult to access structural information for short-lived species, such as intermediates, or for molecular distortion in transition states.[2,3] The spin-Peierls (SP) phase transition is a paramagnetic–diamagnetic transition observed in organic radical crystals at a characteristic temperature, T_{SP}, concomitant with a progressive dimerization between neighboring magnetic species below T_{SP}.[4] The SP transition may be regarded as chemical bond formation in organic radical crystals. Thus, X-ray crystal structure analyses of a dimerization process in the SP system may provide structural information on a chemical bond-formation process. Herein, we describe the magnetic properties and detailed crystal structure analysis of an organic radical magnet, BBDTA·$InBr_4$ (**1**, BBDTA = benzo[1,2-*d*:4,5-*d*′]bis(1,3,2-dithiazole)). We present the SP-like transition of this material at the higher temperature of 250 K and the temperature dependence of structural details on its dimerization process.

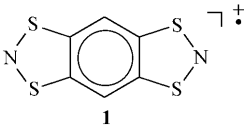

1

Figure 1 shows the temperature dependence of the paramagnetic susceptibility of BBDTA·$InBr_4$ over the temperature range 10–400 K. The open squares show the original susceptibility data. At high temperatures, this material is a paramagnet with intermolecular antiferromagnetic interactions. Near 250 K, the paramagnetic susceptibility (χ_p) gradually decreases to a value close to zero below 100 K, suggesting typical SP-like behavior and dimer formation.

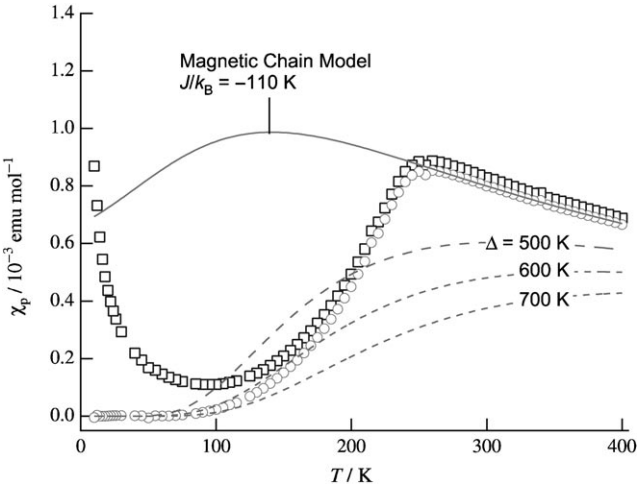

Figure 1. Temperature dependence of the paramagnetic susceptibility, χ_p, in BBDTA·$InBr_4$ (**1**).

Below 100 K, the original susceptibility increases with decreasing temperature. This increase in susceptibility is due to the Curie term from lattice defects and/or magnetic impurities that are not intrinsic in the material. The open circles (Figure 1) correspond to the corrected data, χ_p, that were obtained by subtracting the contribution of the Curie term, $0.0088/T$ emu mol^{-1}, from the original data. The paramagnetic susceptibility above 270 K could be reproduced by using the theoretical equation for the one-dimensional magnetic-chain model [Eq. (1)]:[5]

$$\chi_p = \frac{C}{T}\frac{1 + 0.5998\,y + 1.20376\,y^2}{1 + 1.9862\,y + 0.68854\,y^2 + 6.0626\,y^3} \quad (1)$$

where C is the Curie constant, $y = |J|/k_B T$, J is the intrachain exchange coupling constant, and k_B is Boltzmann's constant. The magnetic parameters, such as the constants $C = 0.366$ emu K mol^{-1} and $Jk_B = -109$ K, were estimated by curve fitting (Figure 1). We could not reproduce the low-temperature magnetic behavior using the theoretical equation of the paramagnetic susceptibility for the magnetic dimer [Eq. (2)],[6]

$$\chi_p = \frac{C}{T}\frac{3}{3 + \exp(\Delta/k_B T)} \quad (2)$$

where Δ expresses a singlet–triplet energy gap. The curves for the energy gap $\Delta = 500$, 600, and 700 K are shown in Figure 1.

[*] Prof. Dr. W. Fujita, Prof. Dr. K. Kikuchi
Department of Chemistry, Tokyo Metropolitan University
Minami-osawa 1-1, Hachioji, Tokyo 192-0367 (Japan)
Fax: (+81) 42-677-2535
E-mail: fujitaw@tmu.ac.jp
Prof. Dr. K. Awaga
Research Center for Materials Science, Nagoya University
Furo-cho, Chikusa-ku, Nagoya 464-8602 (Japan)

[**] This work was partially supported by the Kurata Memorial Hitachi Science and Technology Foundation and the Tokuyama Science Foundation. We thank Seiichi Kagoshima, Keiichiro Ogawa, and Toshiki Sugai for helpful discussions, Mikio Yamasaki for his help in X-ray structural analyses, and Neil Robertson for checking this manuscript.

Supporting information for this article is available on the WWW under http://dx.doi.org/10.1002/anie.200803249.

InterScience
© 2008 Wiley-VCH Verlag GmbH & Co. KGaA, Weinheim

It is apparent that the strength of the chemical bond between neighboring $BBDTA^+$ cations or a singlet–triplet energy gap in the dimer depends on temperature, which is a characteristic of the SP system.

Figure 2 shows the crystal structure, and schematic representations of $BBDTA{\cdot}InBr_4$ at 115 and 270 K. Figure 2a presents the molecular alignment in $BBDTA{\cdot}InBr_4$ crystals, in which a $BBDTA^+$ radical cation directly coordinates to the

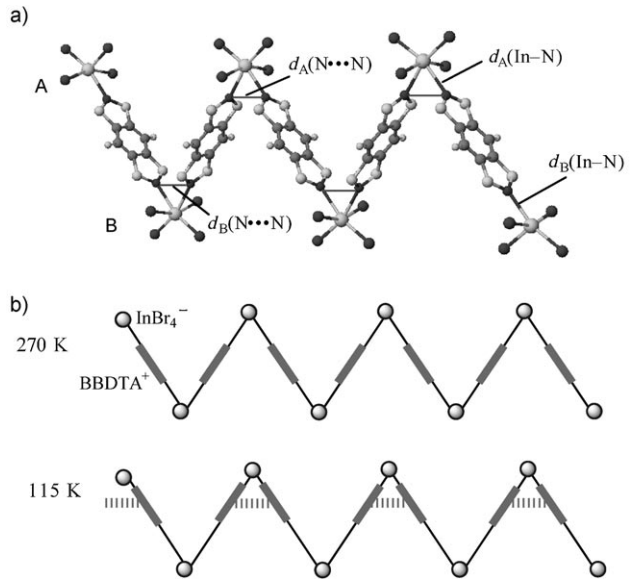

Figure 2. a) A molecular model of the coordination-polymer structure of **1**. b) Schematic representation of the structures at 270 and 115 K.

indium atom of the $InBr_4^-$ unit using the nitrogen atom of the SNS ring, whereby a one-dimensional coordination polymer along the *c* axis is formed. The two $BBDTA^+$ cations occupy the *cis* positions, with In–N bond lengths d_A(In-N) and d_B(In-N) of 2.684(7) Å at 270 K. These distances, however, are longer than the average distance reported for other In–N complexes (2.2 Å),[7] which indicates that the In–N bonds in this material are weaker and more flexible than that in other analogous complexes. At 270 K, short distances, d_A(N···N) and d_B(N···N), of 3.168(11) Å are present between the neighboring $BBDTA^+$ units in the chain. Thus, the structure can be viewed as a 1D antiferromagnetic network that forms by interatomic N···N contacts.

X-ray crystal analyses show that this material undergoes a structural transformation below T_{SP}. The space group changed from *Cmcm* at 270 K to *Pmnm* at 115 K. In the high-temperature phase, the In–N bonds in the regions A and B are equivalent (Figure 2a), whereas those in the low-temperature phase are not. The In–N bond length on the A side, d_A(In-N) is 2.455(10) Å, whereas that on the B side, d_B(In-N) is 2.887(10) Å. Thus, the phase transition causes the In–N coordination bonds to shorten on the A side and the bonds to elongate on the B side, compared with that at 270 K. Furthermore, the N···N distances in regions A and B (2.899 (16) Å and 3.283(17) Å) are nonequivalent. In particular, d_A(N···N) is shorter than the sum of van der Waals radii of two nitrogen atoms, suggesting a very strong intermolecular interaction.

Figure 2b illustrates the structural aspects of this phase transition. At 270 K, $BBDTA^+$ cations are located exactly halfway between the two $InBr_4^-$ units and form a one-dimensional regular array of the radical cations in the polymer chain. At 115 K, $BBDTA^+$ cations approach the indium atoms on the A side and may form a dimer using the shorter N···N interaction that results in a large overlap between the magnetic orbitals of the radical units and a strong antiferromagnetic interaction, leading to diamagnetism at the low temperature.

SP transitions have been found in several organic compounds.[8–12] These materials have the stacking column structure of planar molecules. The transition temperature in $BBDTA{\cdot}InBr_4$, however, is much higher than those in other organic materials,[12] which is probably associated with the nature of the In–N bond. We believe that the high transition temperature is due to the longer In–N bond observed in this coordination polymer, which affords a certain amount of structural flexibility and may thus diminish the loss of lattice energy in the phase transition.

The present phase transition exhibited not only unique lattice dimerization, but also remarkable structural changes in the $BBDTA^+$ molecular shape. Figure 3 shows a structural

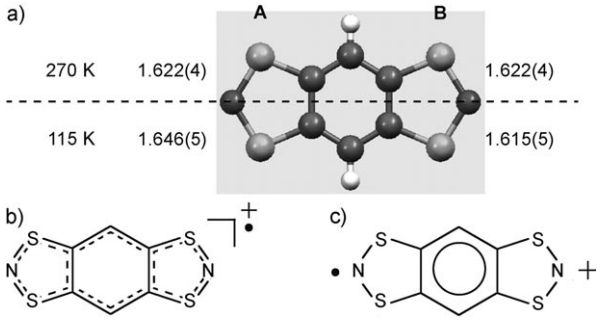

Figure 3. Structural aspects of a $BBDTA^+$ unit in **1**: a) A molecular model showing the S–N bond lengths at 270 and 115 K. Schematic representations of the $BBDTA^+$ unit at b) 270 K and c) 115 K.

model and a schematic representation of the $BBDTA^+$ units at 115 and 270 K. In Figure 3a, the left and right rings correspond to those that are near the A and B sides, respectively (Figure 2a). At 270 K, the S–N bonds on the two SNS rings are all 1.622(4) Å (Figure 3a). At 115 K, the right and left SNS rings became nonequivalent: the S–N bond lengths of the right and left rings are 1.646(5) Å and 1.615(5) Å, respectively. It is known that the S–N bond length and the electric charge on the SNS ring are related.[13,14] In the neutral radical state of the dithiazolyl radicals, the bond distance in S–N is approximately 1.64–1.65 Å. The S–N bond length is 1.62–1.63 Å for a charge of +0.5 per ring, which corresponds to the monocationic state $BBDTA^+$, and about 1.60 Å for the cationic state with +1 per ring. On the basis of this relationship, we can roughly estimate the spin and charge distributions on the two SNS rings of $BBDTA^+$ (Figures 3b, c). At 270 K, the spin and charge-density distributions of the

 © 2008 Wiley-VCH Verlag GmbH & Co. KGaA, Weinheim

right and left rings are identical, judging from the bond lengths and crystal symmetry. At 115 K; however, the S–N bond lengths of the left ring are close to that of the neutral radical state, and the structure of the right ring closely resembles that of the cationic state (Figure 3c). Thus, the spin and charge distribution on the $BBDTA^+$ unit become unsymmetrical below T_{SP}. Such a structural aspect is similar to a characteristic structural form of the distonic radical cations[15] that are reaction intermediates observed during the formation of cationic radical species in gaseous phase. As a result of the asymmetry, dimerization occurs between the neighboring spin-rich rings near the A side.

X-ray analyses of this material at various temperatures below 250 K (T_{SP}) were carried out to validate the dimerization process. Figure 4 shows the temperature dependence of

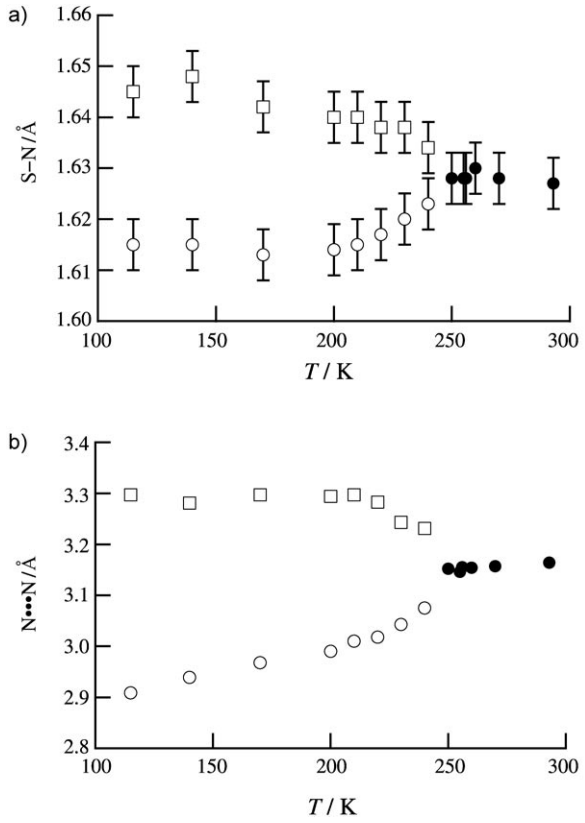

Figure 4. Temperature dependence of structural parameters in a crystal of **1**: a) S–N bond lengths and b) interatomic N···N distances. The two different bond lengths and distances in S–N and N···N, respectively, are represented by □ and ○.

the S–N bond lengths in the $BBDTA^+$ cation and the intermolecular N···N distances between neighboring $BBDTA^+$ cations in the coordination chain. The S–N bond lengths correspond to the charge state of the SNS rings, and the N···N distances represent the extent of dimerization between $BBDTA^+$ cations. Figure 4a shows the temperature dependence of the S–N bond lengths. Above T_{SP}, there is only one kind of S–N bond, suggesting a monocationic state. Below T_{SP}, two different bond lengths are observed. One S–N bond shortens and approaches a value typical for the bond length of the cationic state, whereas the other is elongated and corresponds to that of the neutral radical state. This change in the bond length suggests that disproportionation of spin and charge distributions proceed as a function of temperature. The change in the interatomic N···N distances (Figure 4b) shows a temperature dependence similar to that of the S–N bond length. Below T_{SP}, there were two kinds of N···N distances, of which one monotonically decreases with decreasing temperature, and the other N···N distance increases with lowering of temperature. The shorter N···N distance corresponds to the dimer bond. In this material, lattice dimerization and increase of a singlet–triplet energy gap occurrs gradually as a function of temperature. Thus, the magnetic behavior does not obey the magnetic dimer model[6].

In summary, magnetic and structural studies confirmed the SP-like transition and lattice distortion of the cyclic thiazyl radical $BBDTA{\cdot}InBr_4$. This material did not have the traditional stacking structure of a planar organic radical molecule, but rather a one-dimensional coordination polymer structure. Lattice dimerization of **1** below T_{SP} was accompanied by elongation and contraction of the two In–N bonds between the organic radical unit and $InBr_4$ unit. We demonstrated that strength of chemical bond in the dimer below T_{SP} correlated to the decrease of the N···N distance. Disproportionation of the spin and electric charge distribution on the organic radical unit similar to a distonic ion was also observed. Finally, this work demonstrates that structural analyses of the various SP systems may yield important information on the molecular structures of reaction species in a transition state.

Experimental Section

$BBDTA{\cdot}InBr_4$ (**1**): $BBDTA{\cdot}FeCl_4{\cdot}CH_3CN$[14a,b] (2.05 g) was mixed with tetra(*n*-butyl)ammonium bromide (2.10 g) in acetonitrile (200 mL). A brown precipitate, BBDTA·Br, was obtained, which was washed three times with dichloromethane and dried under vacuum, and was allowed to react with $InBr_3$ (1.4 g) for four hours in acetonitrile (200 mL) under nitrogen atmosphere. The color of the solution gradually changed to deep blue-green, and $BBDTA{\cdot}InBr_4$ was obtained as a blue-green powder by filtration and subsequent evaporation of the remaining solvent. Single crystals were grown from an acetonitrile solution at −3 °C.

Magnetic measurements were carried out on a SQUID (Quantum Design MPMS XL) magnetometer. The experimental raw data were corrected for diamagnetism.

X-ray diffraction data were collected with graphite-monochromated $Mo_{K\alpha}$ ($\lambda = 0.71073$ A) radiation on a RIGAKU Mercury CCD diffractometer. All the structures were solved by direct methods using the SIR90 and SIR2004 program, and refined by successive differential Fourier syntheses and a full-matrix least-squares procedure using the SHELXL-97 program.[16] Anisotropic thermal factors were applied to all non-hydrogen atoms. Crystal data for $BBDTA{\cdot}InBr_4$ at 270 K: $C_6Br_4H_2In_1N_2S_4$, $M_r = 664.80$, orthorhombic, *Cmcm*, $a = 9.299(5)$, $b = 10.608(5)$, $c = 14.432(7)$ Å, $V = 1423.5(12)$ Å^3, $Z = 4$, $R_1 = 0.0370$ ($\sigma > 2.0$), $wR_2 = 0.1155$ (all data), $S = 1.004$ (all data). Crystal data at 115 K: orthorhombic, *Pmmn*, $a = 14.247(5)$, $b = 9.260(3)$, $c = 10.638(4)$ Å, $V = 1403.4(9)$ Å^3, $Z = 4$, $R_1 = 0.0403$ ($\sigma > 2.0$), $wR_2 = 0.0869$ (all data), $S = 1.015$ (all data). CCDC-698635 (at 270 K) and CCDC-698636 (at 115 K) contain the supplementary crystallographic data for this paper. These data can be obtained free

 © 2008 Wiley-VCH Verlag GmbH & Co. KGaA, Weinheim

of charge from The Cambridge Crystallographic Data Centre via www.ccdc.cam.ac.uk/data_request/cif.

Received: July 4, 2008
Published online: October 23, 2008

Keywords: distonic cations · magnetic properties · radicals · spin-Peierls phase transition · structure elucidation

[1] J. C. Polanyi, A. H. Zewail, *Acc. Chem. Res.* **1995**, *28*, 119 – 132.
[2] J. D. Dunitz, *X-Ray Analysis and the Structure of Organic Molecules*, VCH, Basel, **1995**.
[3] a) P. Baum, D.-S. Yang, A. H. Zewail, *Science* **2007**, *318*, 788 – 792; b) D. Shorokhov, A. H. Zewail, *Phys. Chem. Chem. Phys.* **2008**, *10*, 2879 – 2893.
[4] J. W. Bray, L. V. Interrante, I. S. Jacobs, J. C. Bonner, *Extended Linear Chain Compounds*, *Vol. 3* (Ed: J. S. Miller), Prenum, New York, **1983**, pp. 353 – 415.
[5] J. C. Bonner, M. E. Fisher, *Phys. Rev.* **1964**, *135*, A640 – A658.
[6] B. Bleany, K. D. Bowers, *Proc. R. Soc. London Ser. A* **1952**, *214*, 451 – 465.
[7] T. Grabowy, K. Merzweiler, *Z. Anorg. Allg. Chem.* **2000**, *626*, 736 – 740.
[8] J. W. Bray, H. R. Hart, Jr., L. V. Interrante, I. S. Jacobs, J. S. Kasper, G. D. Watkins, S. H. Wee, *Phys. Rev. Lett.* **1975**, *35*, 744 – 747.
[9] S. Huizinga, J. Kommandeur, G. A. Sawatzky, B. T. Thole, K. Kopinga, W. J. M. de Jongh, J. Roos, *Phys. Rev. B* **1979**, *19*, 4723 – 4732.
[10] K. Mukai, N. Wada, J. B. Jamali, N. Achiwa, Y. Narumi, K. Kindo, T. Kobayashi, K. Amaya, *Chem. Phys. Lett.* **1996**, *257*, 538 – 544.
[11] Y. Nakazawa, A. Sato, M. Seki, K. Saito, K. Hiraki, T. Takahashi, K. Kanoda, M. Sorai, *Phys. Rev. B* **2003**, *68*, 085112.
[12] W. Fujita, K. Awaga, R. Kondo, S. Kagoshima, *J. Am. Chem. Soc.* **2006**, *128*, 6016 – 6017.
[13] Y. Umezono, W. Fujita, K. Awaga, *J. Am. Chem. Soc.* **2006**, *128*, 1084 – 1085.
[14] a) G. Wolmershäuser, G. Wortman, M. Schnauber, *J. Chem. Res. Synop.* **1988**, 358 – 359; b) E. G. Awere, N. Byeford, R. C. Haddon, S. Parsons, J. Passmore, J. V. Waszczak, P. S. White, *Inorg. Chem.* **1990**, *29*, 4821 – 4830; c) T. M. Barclay, A. W. Cordes, R. H. de Laat, J. D. Goddard, R. C. Haddon, D. Y. Jeter, R. C. Mawhinney, R. T. Oakley, T. T. M. Palstra, G. W. Patenaude, R. W. Reed, N. P. C. Westwood, *J. Am. Chem. Soc.* **1997**, *119*, 2633 – 2641.
[15] K. M. Stirk, L. K. M. Kiminkinen, H. I. Kenttämaa, *Chem. Rev.* **1992**, *92*, 1649 – 1665.
[16] G. M. Sheldrick, Program for the Refinement of Crystal Structures, University of Göttingen, Germany, **1997**.

 © 2008 Wiley-VCH Verlag GmbH & Co. KGaA, Weinheim